Classical Keggin Intercalated into Layered Double Hydroxides: Facile Preparation and Excellent Performance for Knoevenagel Condensation

Yueqing Jia,[a] Yanjun Fang,[b] Yingkui Zhang,[b]* Haralampos N. Miras[c]* and Yu-Fei Song*[a]

Abstract: The family of polyoxometalate (POM) intercalated layered double hydroxides (LDHs) composite materials has shown great promise for the design of functional materials with numerous applications. It is known that intercalation of the classical Keggin polyoxometalate (POM) of $[PW_{12}O_{40}]^{3-}$ (PW_{12}) into layered double hydroxides (LDHs) is very unlikely to take place by conventional ion exchange methods due to spatial and geometrical restrictions. In this paper, such intercalated compound of $Mg_{0.73}Al_{0.22}(OH)_2[PW_{12}O_{40}]_{0.04}\cdot 0.98H_2O$ (Mg_3Al-PW_{12}) has been successfully obtained by adopting a spontaneous flocculation method. The Mg_3Al-PW_{12} has been fully characterized using a wide range of methods (XRD, SEM, TEM, XPS, EDX, XPS, FT-IR, NMR, BET). XRD patterns of Mg_3Al-PW_{12} exhibit no impurity phase usually observed next to the (003) diffraction peak. Subsequent application of the Mg_3Al-PW_{12} as catalyst in Knoevenagel condensation reactions of various aldehydes and ketones with Z–CH_2-Z' type substrates (ethyl-cyanoacetate and malononitrile) at 60 °C in mixed solvents ($V_{i\text{-}propanol}$:V_{water} = 2 : 1) demonstrated highly efficient catalytic activity. The synergistic effect between the acidic and basic sites of the Mg_3Al-PW_{12} composite proved to be crucial for the efficiency of the condensation reactions. Additionally, the Mg_3Al-PW_{12} catalysed Knoevenagel condensation of benzaldehyde with ethyl cyanoacetate demonstrated the highest turnover number (TON) of 47980 reported so far.

Introduction

Polyoxometalates (POMs) are a class of molecular anionic metal oxides mainly groups V and VI. They are constructed *via* a condensation reaction between their metal oxide polyhedra (MO_x: M = W^{VI}, Mo^{VI}, V^{V}, Nb^{V}, Ta^{V}, *etc.*, and x = 4-7) bridged together in a corner-, edge-, or rarely in a face-shared fashion.[1-3] POMs found to be very attractive systems due to their fascinating properties which can be finely tuned by appropriate choice of metal ion(s), heteroatoms and counter ions.[4-6] One the POMs' important properties is their superior catalytic performance in numerous processes which has been exploited in industrial processes.[7-13] However, the industrial application of POM-based homogeneous catalytic systems has been largely restricted by the poor solubility of POMs in common organic solvents due to their crystalline nature, high negative charge, low energy lattice[14], contamination/separation and decomposition issues. Consequently, design of POM-based heterogeneous catalysts is a potentially alternative way to overcome the above limitations and fine control of the POM-based material's functionality. In an effort to develop POM-based heterogeneous catalysts, the solidification and immobilization are the two strategies that have been widely adopted.[15-17]

Layered double hydroxides (LDHs) or hydrotalcite-like compounds are a large family of two-dimensional (2D) anionic clay materials represented by the general formula of $[M^{2+}_{1-x}M^{3+}_x(OH)_2]^{x+}[A_{x/n}]^{n-}\cdot mH_2O$, where M^{2+} and M^{3+} are di- and trivalent metal cations, A^{n-} is the counteranion and x = 0.17-0.33 defines the $M^{3+}/(M^{2+}+M^{3+})$ ratio.[18-20] The interlayer anions are linked within the positively charged host layer by means of electrostatic forces and hydrogen bonding interactions *via* the interlayer water molecules or hydroxyl groups.[21,22] LDHs can provide a flexible confined space that can be adjusted by changing the size and the structure of a guest molecules. The flexible interlayer space can not only host small-sized moieties, but also accommodate bulkier species that are difficult or even impossible to enter a material's rigid pores of fixed dimensions.[23,24] Therefore, LDHs are ideal support for larger species of various structures such as POM anions.

The POM-LDHs nanocomposites *via* the intercalation of POM species into LDHs have attracted wide interest as they have shown great advantages over both traditional LDH and POMs compounds.[25-28] However, the relevant intercalation process faces two serious challenges: 1) it is almost impossible to obtain POM-LDHs nanocomposites with no impurity using traditional synthetic methods such as co-precipitation, ion-exchange, and two-step ion-exchange method[29,30]; 2) the POMs intercalation is closely related to the geometry, charge and size of POMs.[31] For example, the classical Keggin cluster of PW_{12} with the negative charge below 4 are very unlikely to intercalate into LDHs using the conventional synthetic methods due to the spatial and geometrical considerations of the size of the Keggin ions and the surface area available.[31] Therefore, it is significant to design a new synthetic strategy in order to overcome such spatial and geometrical restriction for the develpment of POM-LDHs functional materials.

Recently, we have successfully prepared the LDHs-POMs of $Mg_{0.77}Al_{0.23}(OH)_2[LnW_{10}O_{36}]_{0.026}$ (Mg_3Al-LnW_{10}, Ln = Eu, Tb and Dy) *via* the spontaneous flocculation method.[32] It is worth noting that the flocculation process not only provides a new way for rational design of new layered materials with precisely controlled nanostructures, but also prevents the leaching of Mg^{2+}/Al^{3+} cations during the intercalation and thereby successfully controls the final Mg^{2+}/Al^{3+} ratio in the Mg_3Al-LnW_{10} (Ln = Eu, Tb, Dy)

[a] Y. Jia, and Prof. Y. F. Song*
State Key Laboratory of Chemical Resource Engineering
Beijing University of Chemical Technology
Beijing 100029 (P. R. China)
Fax: (+86) 10-64431832
E-mail: songyufei@hotmail.com or songyf@mail.buct.edu.cn
[b] Y. Fang, Prof. Y. Zhang*
School of Economics and Management
Beijing University of Chemical Technology
Beijing 100029 (P. R. China)
[c] Dr. H. N. Miras*
WestCHEM, School of Chemistry, University of Glasgow
Glasgow, G12 8QQ, UK. Email: harism@chem.gla.ac.uk

Supporting information for this article is given via a link at the end of the document.

composites. Additionally, the Mg_3Al-LnW_{10} materials have been obtained without the co-precipitation of an impurity phase. To extend the application scope of the spontaneous flocculation method, we have applied this method to explore the classical Keggin cluster of $[PW_{12}O_{40}]^{3-}$ (PW_{12}) into Mg_3Al-LDHs for the first time, which is challenging to achieve using conventional synthetic methods.

In this paper, we have successfully prepared a new member of the POM-LDHs family with the composition $Mg_{0.73}Al_{0.22}(OH)_2[PW_{12}O_{40}]_{0.04}\cdot 0.98H_2O$ (Mg_3Al-PW_{12}) following a spontaneous flocculation method. Application of Mg_3Al-PW_{12} in Knoevenagel condensation of various aldehydes and ketones with methylene compounds (ethyl cyanoacetate and malononitrile) in a mixed solvent medium ($V_{i\text{-propanol}}$:V_{water} = 2 : 1) at 60 °C exhibited an excellent catalytic performance with the highest TON reported so far.

Results and Discussion

The facile and spontaneous flocculation method used for the preparation of the Mg_3Al-PW_{12} can be summarized as follows:[32] the precursor of $[Mg_{0.75}Al_{0.25}(OH)_2](NO_3)_{0.250}\cdot 2H_2O$ (Mg_3Al-NO_3) can be prepared followed an acid-alcohol mixed method reported earlier.[33] The positive nanosheets of $[Mg_{0.75}Al_{0.25}(OH)_2]^{0.25+}$ can be obtained by exfoliation of Mg_3Al-NO_3 in formamide, which can be confirmed to be unilamellar with lateral dimensions of 2-3 μm.[34] The aqueous solution of PW_{12} is then added gradually into the positive Mg_3Al-LDHs nanosheets suspension. Subsequently, the spontaneous flocculation of the positive Mg_3Al-LDHs nanosheets and the negative PW_{12} clusters takes place, followed by the isolation of the Mg_3Al-PW_{12} nanocomposite *via* centrifugation. Note that the acid resistance of the LDHs is much stronger in organic solvents than that in water, which can reduce significantly the co-formation of the impurity phase which can be attributed to the formation of Mg^{2+} rich salt of the POM species. Exploitation of the spontaneous flocculation method gave rise to the successful formation of the Mg_3Al-PW_{12} composite, in contrast to the conventional synthetic methods where previous studies suggested that POM anions with negative charge below 4, such as the PW_{12} cluster, are very unlikely to intercalate into LDHs.

XRD patterns of Mg_3Al-PW_{12} (Fig 1A) show five Bragg diffraction peaks in the range of $3^o < 2\theta < 70^o$, which can be fully indexed to a hexagonal unit cell belonging to the *R-3m* space group of the intercalated PW_{12} cluster. The corresponding basal spacing of *d*(003) has been summarized in Table S1. The gallery height value of 0.93 nm can be obtained by subtracting the thickness of host layer (0.48 nm)[26] from the value of *d*(003) spacing of Mg_3Al-PW_{12}. The gallery height is nearly the same as the diameter of the short axis of PW_{12},[35] indicating that the C_3 axis of PW_{12} anions is perpendicular to the host layers. Thus, the PW_{12} anions are uniformly oriented within the interlayer space of the Mg_3Al-LDHs. Importantly, XRD patterns of the Mg_3Al-PW_{12} do not show the impurity phase usually observed at $2\theta = \sim 11^o$.[32,35] The impurity phase is a common issue for LDHs-POM nanocomposites prepared by traditional ion exchange methods[25] and is often attributed to the co-formation of a Mg^{2+} rich salt.[30] Current experimental results confirm that the Mg_3Al-PW_{12} can be prepared following the reported spontaneous flocculation method without the co-formation of the impurity phase.

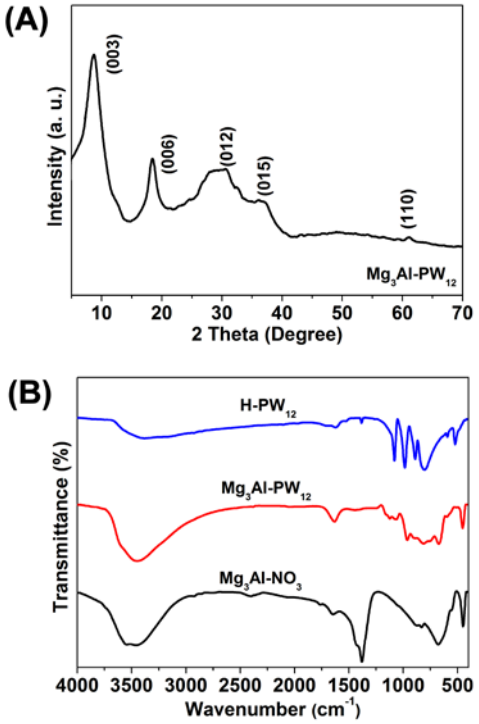

Figure 1. XRD patterns (A) and FT-IR (B) spectrum of Mg_3Al-PW_{12}.

FT-IR spectra of Mg_3Al-PW_{12}, H-PW_{12}, and Mg_3Al-NO_3 are shown in Fig 1B. The sharp and narrow absorption band at 1378 cm^{-1} in the spectrum of Mg_3Al-NO_3 is due to the characteristic stretching vibration of NO_3^- groups.[36] In the case of H-PW_{12}, the strong absorption bands at 1048, 949, 883, 699 and 593 cm^{-1} can be assigned to the P-O, W-O_t, W-O_c-W and W-O_e-W asymmetric stretching vibrations and P-O bending vibration, respectively. For the FT-IR spectrum of Mg_3Al-PW_{12}, the broad band at 3443 cm^{-1} is assigned to the O-H stretching vibration in the brucite-like layers, and it is noted that this absorption is located at much lower frequency than that of Mg_3Al-NO_3 at 3502 cm^{-1}, which might result from the hydrogen bonding between interlayer water and hydroxyl groups of the host layers.[37,38] The characteristic absorption bands for the P-O and W-O shift from 1048, 949, 883, 699 and 593 cm^{-1} in H-PW_{12} to higher frequency at 1050, 951, 885, 701 and 595 cm^{-1} in Mg_3Al-PW_{12}, indicating the presence of electrostatic interactions between the host layers and the guest anions.[27,28] The absorption band at 450 cm^{-1} can be attributed to O-M-O (M = Mg and Al) vibrations in the brucite-like layers of the LDH.[39] Compared with that of Mg_3Al-NO_3, the disappearance of the absorption band at 1378 cm^{-1} for nitrate anions and the presence of the stretching bands of PW_{12} in the FT-IR spectrum of Mg_3Al-PW_{12} indicate the successful formation of Mg_3Al-PW_{12}.

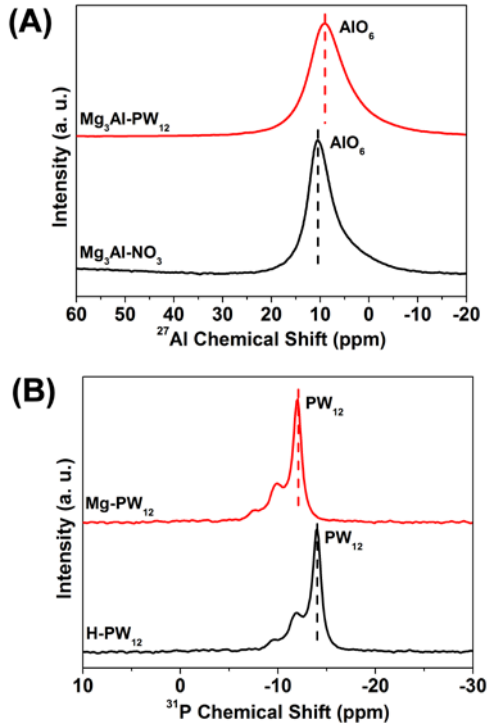

Figure 2. The ^{27}Al- (A) and ^{31}P- (B) NMR spectra of Mg_3Al-PW_{12}.

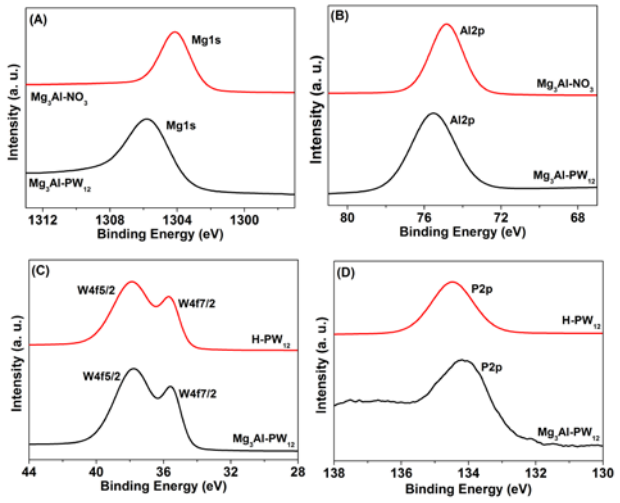

Figure 3. XPS spectra of Mg_3Al-PW_{12}.

Solid state ^{27}Al-NMR and ^{31}P-NMR have been used to probe the local environments of Al^{3+} and P^{5+} centres in the Mg_3Al-PW_{12}. As shown in Figure 2A, the ^{27}Al resonance line positions are very sensitive to the coordination number and are expected to apear within the range of -5 to 15 ppm for octahedral geometry of AlO_6 sites.[40] The ^{27}Al-NMR spectrum of Mg_3Al-NO_3 shows only one peak at 10.50 ppm, which clearly demonstrates that all of the Al^{3+} in Mg_3Al-NO_3 adopt octahedral geometry. Additionally, only one peak centred at 9.15 ppm is also visible in the ^{27}Al-NMR spectrum of the Mg_3Al-PW_{12} composite, demonstrating that all of the Al^{3+} in Mg_3Al-PW_{120} are located in an octahedral environment.

In Figure 2B, one set of signals centred at ´ = -14.18 ppm in the ^{31}P-NMR spectrum of H-PW_{12} is assigned to the PW_{12} anions.[35] Additionally, only one set of signals centred at ´ = -12.03 ppm is observed in the ^{31}P-NMR spectrum of Mg_3Al-PW_{12}. The above solid state NMR results reveal that the structure of both Mg_3Al-LDHs and PW_{12} remain unchanged after the interacalation. The shift of the peaks obseved in the solid state NMR spectra is due to the interactions between the host layers of Mg_3Al-LDHs and the intercalated guest PW_{12}.[32]

The XPS spectra corresponding to Mg core levels of the Mg_3Al-PW_{12} and Mg_3Al-NO_3 are shown in Figure 3A. The binding energy of Mg_{1s} is 1305.9 eV in the Mg_3Al-PW_{12} and 1303.6 eV in Mg_3Al-NO_3. The XPS spectra corresponding to Al core levels of the Mg_3Al-PW_{12} and Mg_3Al-NO_3 are shown in Figure 3B. The binding energy of Al_{2p} is 74.9 eV and 74.6 eV, respectively. The binding energy of $W4f_{7/2}$ and $W4f_{5/2}$ are 35.6 and 37.7 eV in the Mg_3Al-PW_{12}, while 35.7 and 37.9 eV in the H-PW_{12} (Fig 3C). In a similar fashion, the binding energy of P_{2p} is 134.3 eV in the Mg_3Al-PW_{12}, and 134.4 eV in the H-PW_{12} (Figure 3D). The above results reveal that the binding energies of Mg_{1s} and Al_{2p} in the Mg_3Al-PW_{12} are almost the same as those of the Mg_3Al-NO_3. Moreover, the binding energies of $W4f_{7/2}$, $W4f_{5/2}$ and P_{2p} in the Mg_3Al-PW_{12} remain unchanged compared with those of the free H-PW_{12} species. These results reveal that the structures of Mg_3Al-LDHs layers and PW_{12} remain unchanged in the Mg_3Al-PW_{12}.

The thermogravimetric analysis (TGA) curve for the Mg_3Al-PW_{12} is shown in Figure S2. Two weight-loss stages can be observed upon increase of the temperature from 30 to 900 °C. The first weight loss is 9.22% between 30 and 240 °C is attributed to the removal of water molecules (Calcd. $98H_2O$ per Mg_3Al-PW_{12}).The second weight loss step of 10.57% at 240-610 °C can be attributed to the collapse of the layered structure. The molecular formula of Mg_3Al-PW_{12} can be identified as $Mg_{0.73}Al_{0.22}(OH)_2[PW_{12}O_{40}]_{0.04}\cdot 0.98H_2O$ by taking into consideration the TGA and ICP analysis data (Table S8). SEM and TEM images of Mg_3Al-PW_{12} revealed the porous stacking of sheet-like crystallites (Figure S3). The particle sizes of these crystallites fall in the range of 200-400 nm. Moreover, adsorption-desorption studies of the Mg_3Al-PW_{12} composite material, Figure S4, revealed a type I adsorption isotherm at relative lower pressure ($P/P_0 < 0.1$), and an H_3 type N_2 hysteresis loop at relative higher pressure regimes ($P/P_0 > 0.5$), according to the BDDT (Brunauer, Deming, Deming and Teller) classification,[40] indicating the presence of both interlayer micropores and inter-particle mesopores.

Table 1. BET and TPD results of Mg_3Al-PW_{12}.

Entry	Catalyst	Surface Area ($m^2 \cdot g^{-1}$)	Pore Volume ($cm^3 \cdot g^{-1}$)	Pore Size (nm)	Total Acidity (mmol $NH_3 \cdot gcat^{-1}$)[a]	Total Basicity (mmol $CO_2 \cdot gcat^{-1}$)[b]
1	Mg_3Al-PW_{12}	18.5	0.041	4.8	0.94	1.13
2	Reused Mg_3Al-PW_{12}	18.1	0.041	4.8	0.93	1.15

[a] The amount of acid sites were calculated by quantifying the desorbed NH_3 from NH_3-TPD. [b] The amount of basic sites were calculated by quantifying the desorbed CO_2 from CO_2-TPD.

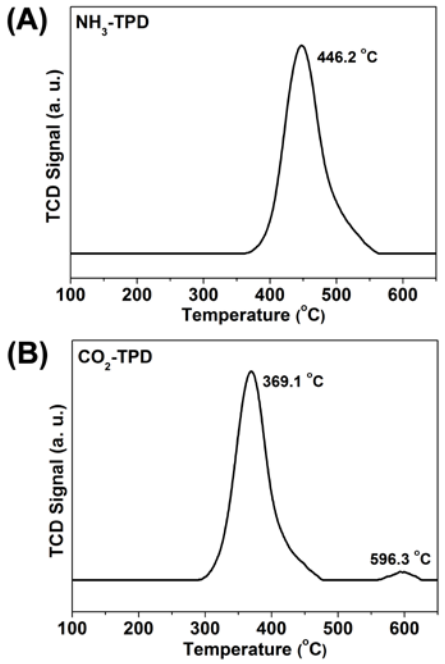

Figure 4. NH_3 (A) and CO_2 (B) TPD profiles of Mg_3Al-PW_{12}.

Temperature-programmed desorption of ammonia (NH_3-TPD) demonstrate that the Mg_3Al-PW_{12} exhibits the NH_3 desorption peak at 446.2 °C in Figure 4A, which corresponds to the NH_3 molecules adsorbed on strong acidic sites (Brónsted and Lewis acidic sites) of Keggin POM species. Temperature-programmed desorption of carbon dioxide (CO_2-TPD) demonstrates that the Mg_3Al-PW_{12} gives a CO_2 desorption peak centred at 369.1 °C in Figure 4B, which corresponds to the CO_2 molecules adsorbed on medium basic sites of Mg_3Al-LDHs. The total acidity and basicity of the Mg_3Al-PW_{12} determined by NH_3-TPD and CO_2-TPD measurements have been summarized in Table 1. The above data confirm the amphoteric behaviour of the Mg_3Al-PW_{12} catalyst. The co-existence of both types of sites will prove to be crucial for the superior performance of the catalyst, as it is discussed below.

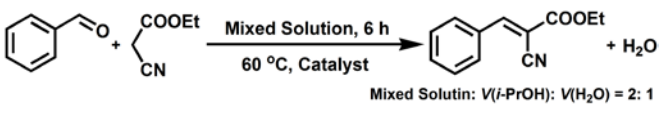

Table 2. Effect of different catalysts on Knoevenagel condensation of benzaldehyde with ethyl cyanoacetate at 60 °C in mixed solution $V_{i\text{-propanol}}$: V_{water} = 2: 1.[a]

Entry	Catalyst	Yield (%)
1	Mg_3Al-PW_{12}	>99.9
2	H-PW_{12}	1
3	Na-PW_{12}	1
4	Mg_3Al-NO_3	20
5	Mg_3Al-NO_3+H-PW_{12}	10
6	Na_2WO_4	2
7	Na_2HPO_4	1
8	NaH_2PO_4	1
9	WO_3	1
10	None	1

[a] Reaction conditions: benzaldehyde (1 mmol), catalyst (3.0 mol% to benzaldehyde based on W), ethyl cyanoacetate (1.5 mmol), 0.6 ml mixed solution $V_{i\text{-propanol}}$:V_{water} = 2: 1, 60 °C, 6 hours. Yields were determined by GC analysis using reference standards. Assignments of corresponding products were analyzed by ^{1}H-NMR and ^{13}C-NMR.

Knoevenagel condensation of carbonyl compounds with active methylene compounds is one of the most significant reactions for C-C bond formation, which has been widely applied in the synthesis of important intermediates or products for pharmaceuticals and calcium antagonists, and polymers.[41-43] Knoevenagel condensation is a base-catalyzed reaction. Initially, Knoevenagel condensation of benzaldehyde with ethyl cyanoacetate catalyzed by Mg_3Al-PW_{12} has been carried out at 60 °C in mixed solution ($V_{i\text{-propanol}}$:V_{water} = 2 : 1), during which an excellent yield of > 99.9% was obtained (Table 2, Entry 1). Efforts to catalyze the same reaction mixture using the Keggin POMs on their own, $H_3PW_{12}O_{40}$ (H-PW_{12}) and $Na_3PW_{12}O_{40}$ (Na-PW_{12}), were not effective (Entries 2 and 3). Additionally, catalyis of the reaction mixture by the Mg_3Al-NO_3 gave a very low yield of 20% (Entry 4). Further control experiments involved utilization of the physical mixture of Mg_3Al-NO_3 and H-PW_{12} which gave an even worse yield (10%) than that of Mg_3Al-NO_3 on its own (Entry 5). Moreover, neither of the individual components of the POM structure, Na_2WO_4, Na_2HPO_4, NaH_2PO_4 and WO_3 gave any catalytic performance (Entries 6-9) and as we suspected the reaction cannot proceed in the absence of a catalyst (Entry 10).

All the above experimental results in Table 2 confirm furhter that the Mg_3Al-PW_{12} composite material is a highly effective catalyst for Knoevenagel condensation reactions. Taking into consideration the previously reported results and our experimental data discussed herein, becomes clear that the synergistic effect between the LDHs layers and the PW_{12} anions in Mg_3Al-PW_{12} composite material is crucial for the efficient promotion of the Knoevenagel condensation.

The effect of various solvent media on the Knoevenagel condensation of benzaldehyde with ethyl cyanoacetate was investigated (Table S5). The results revealed that the best performance was obtained in a mixed solution of $V_{i\text{-propanol}}$:V_{water} = 2 : 1. Therefore, the Knoevenagel condensation of various aldehydes and ketones with ethyl cyanoacetate and malonitrile was investigated in mixed solution medium $V_{i\text{-propanol}}$:V_{water} = 2 : 1.

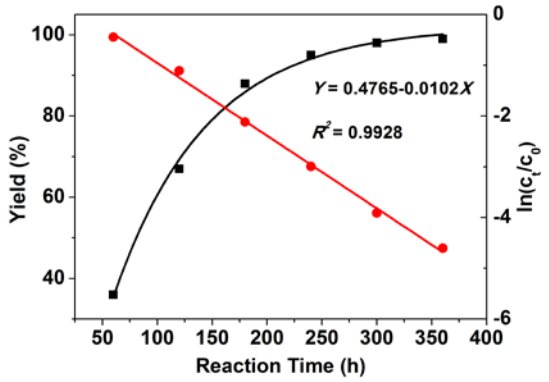

Figure 5. Kinetic profiles of the Knoevenagel condensation of benzaldehyhde with ethyl cyanoacetate catalyzed by Mg_3Al-PW_{12} (black line: yield of corresponding products; red line: $\ln(C_t/C_0)$).

In order to obtain the kinetic parameters for Knoevenagel condensation of benzaldehyde with ethyl cyanoacetate, catalytic experiments have been performed using a reaction mixture ratio of benzaldehyde : ethyl cyanoacetate : PW_{12} = 401 : 602 : 1 at 60 ^{o}C in a mixed solvent medium of $V_{i\text{-propanol}}$:V_{water} = 2 : 1. The yield and $\ln(C_t/C_0)$ are plotted against the reaction time in Figure 5, where C_0 and C_t are initial corresponding product concentration and corresponding product concentration at time t, respectively. The linear fit of the data reveals that the catalytic reaction exhibits pseudo-first-order kinetics for the Knoevenagel condensation (R^2 = 0.9928). The rate constant k of the Knoevenagel condensation was determined to be 0.0102 min^{-1} based on the Equations 1 and 2. Knoevenagel condensation of benzaldehyde with ethyl cyanoacetate could be completed with a yield of >99.9% in 6 hours. Thus, the catalyst of Mg_3Al-PW_{12} exhibits high catalytic efficiency for Knoevenagel condensations, whilst the catalytic reaction follows pseudo-first-order kinetics with >99.9% selectivity of the corresponding products.

$$-dCt / dt = kCt \quad (1)$$

$$\ln(Co / Ct) = kt \quad (2)$$

As shown in Figure 6A, the yield is quite low at 25 ^{o}C using Mg_3Al-PW_{12} as catalyst for Knoevenagel condensation of benzaldehyde with ethyl cyanoacetate in $V_{i\text{-propanol}}$:V_{water} = 2 : 1. However, increase of the reaction temperature from 25 to 60 ^{o}C, the yield increases from 65% to >99.9%, whilst the yield remains unchanged upon further increase of the temperature. Yield and $\ln(C_t/C_0)$ are plotted against the reaction time at 25, 40, 50, 60 and 70 ^{o}C, (Figure S5). C_0 and C_t are the concentrations of the corresponding product initially and at time t, respectively. The linear fit of the data reveals that the catalytic reaction follows pseudo-first-order kinetics at 25, 40, 50, 60 and 70 ^{o}C, respectively. The calculated activation energy (E_a) using the Arrhenius equation for Knoevenagel condensation of benzaldehyde with ethyl cyanoacetate by Mg_3Al-PW_{12} is 33.3 $kJ{\cdot}mol^{-1}$.

Knoevenagel condensation of various aldehydes and ketones with ethyl cyanoacetate catalyzed by Mg_3Al-PW_{12} has been investigated at 60 ^{o}C in $V_{i\text{-propanol}}$:V_{water} = 2 : 1. All the corresponding products were obtained in high yields. More specifically, for aromatic aldehydes (benzaldehyde), Methyl substituted aromatic aldehydes (2-methylbenzaldehyde, 3-methylbenzaldehyde, and 4-methylbenzaldehyde) and methoxy-substituted aromatic aldehydes (2-methoxylbenzaldehyde, 3-methoxybenzaldehyde, and 4-methoxybenzaldehyde), can all be converted to the corresponding products at high yields of >99.9% (Table 3, Entry 1), 92%, 99%, and 97% (Entries 2-4) and 92%, >99.9%, and 99% (Entries 5-7), respectively.

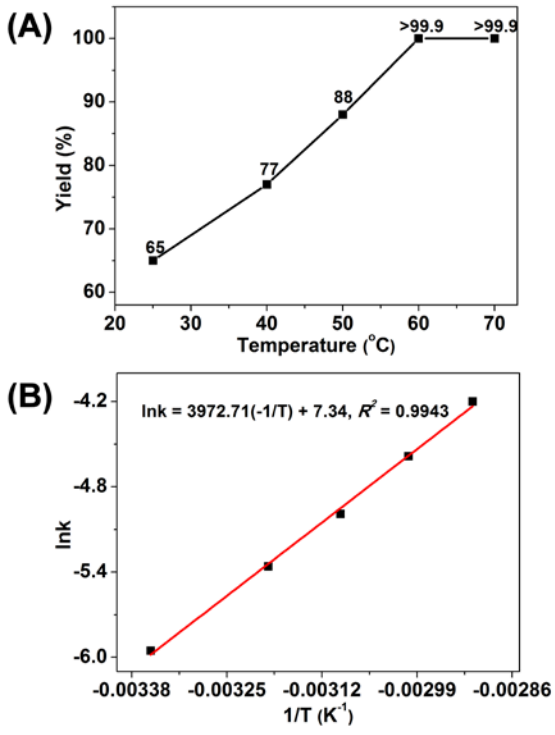

Figure 6. Effect of T on Knoevenagel condensation of benzaldehyde with ethyl cyanoacetate (A) and the plot lnk(T) vs (-1/T) (B). benzaldehyde (1 mmol), Mg_3Al-PW_{12} (0.25 mol% to benzaldehyde based on PW_{12}), ethyl cyanoacetate (1.5 mmol), 0.6 ml mixed solution $V_{i\text{-propanol}}$:V_{water} = 2 : 1), 6 hours.

Table 3. Knoevenagel condensation of benzaldehyde with ethyl cyanoacetate catalyzed by Mg_3Al-PW_{12} at 60 °C in mixed solution $V_{i\text{-propanol}}$:V_{water} = 2 : 1.[a]

Entry	Donor	Acceptor	Product	Yield (%)
		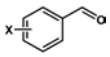	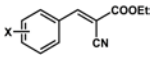	
1		X = H	X = H	>99.9
2		X = 2-Me	X = 2-Me	92
3		X = 3-Me	X = 3-Me	99
4		X = 4-Me	X = 4-Me	97
5		X = 2-MeO	X = 2-MeO	92
6		X = 3-MeO	X = 3-MeO	>99.9
7		X = 4-MeO	X = 4-MeO	99
8		X = 2-Cl	X = 2-Cl	98
9		X = 3-Cl	X = 3-Cl	>99.9
10		X = 4-Cl	X = 4-Cl	>99.9
11		X = 2-Br	X = 2-Br	99
12		X = 3-Br	X = 3-Br	>99.9
13	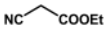	X = 4-Br	X = 4-Br	>99.9
14		X = 2-NO_2	X = 2-NO_2	>99.9
15		X = 3-NO_2	X = 3-NO_2	>99.9
16		X = 4-NO_2	X = 4-NO_2	>99.9
17			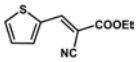	>99.9
18			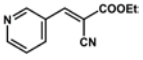	>99.9
			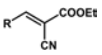	
19		R = *n*-C_5H_{11}	R = *n*-C_5H_{11}	99
20		R = *n*-C_6H_{13}	R = *n*-C_6H_{13}	86
21		R = *n*-C_7H_{15}	R = *n*-C_7H_{15}	82
22		R = *n*-C_8H_{17}	R = *n*-C_8H_{17}	76
23		R = *n*-C_9H_{19}	R = *n*-C_9H_{19}	71
24			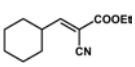	98

[a] Reaction conditions: benzaldehyde (1 mmol), Mg_3Al-PW_{12} (0.25 mol% to substrate based on PW_{12}), ethyl cyanoacetate (1.5 mmol), 0.6 ml mixed solution $V_{i\text{-propanol}}$:V_{water} = 2 : 1, 60 °C, 6 hours. Yields were determined by GC analysis using reference standards. Assignments of corresponding products were analyzed by ^{1}H-NMR and ^{13}C-NMR.

In an effort to explore fully the performance of the catalyst, we used electron-withdrawing substituted aromatic aldehydes as substrates (2-chlorobenzaldehyde, 3-chloro benzaldehyde, 4-chlorobenzaldehyde, 2-bromobenzaldehyde, 3-bromobenzaldehyde, 4-bromobenzaldehyde, 2-nitrobenz aldehyde, 3-nitrobenzaledhyde and 4-nitrobenzaldehyde) where we obtained equally high yields, 98%, >99.9%, >99.9%, 99%, >99.9%, >99.9%, >99.9%, >99.9%, and >99.9%, respectively (Entries 8-16). Knoevenagel condensation of thiophene-2-carboxaldehyde and pyridine-3-carboxaldehyde gave us also excellent yields of both above 99.9% (Entries 17 and 18).

Finally, the Knoevenagel condensation of aliphatic aldehydes (hexanal, heptanal, octanal, nonanal, and decanal) gave us a range of high to very good yields (99%, 86%, 82%, 76%, and 71%; Entries 19-23) whilst the cyclic aliphatic aldehyde of cyclohexanecarboxaldehyde proceeds efficiently with a high yield of 98% (Entry 24). The above results suggest that the catalytic performance is excellent when the substrate is electron-donating /withdrawing substituted aromatic aldehyde. The observed small decrease of the catalytic activities in the case of alkyl aldehydes can be attributed to the increased hydrophobicity as a function of the length of the alkyl chain. It is worth noting that all the resulting products show excellent E/Z ⩾ 99/1.

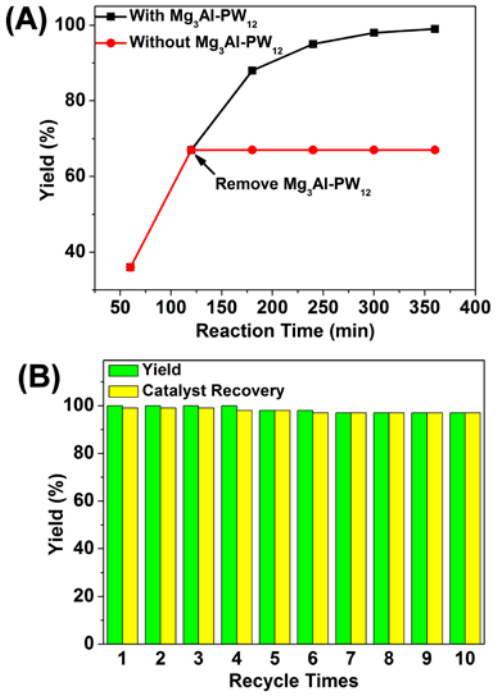

Figure 7. Recycling experiments of Mg_3Al-PW_{12} for Knoevenagel condensation of benzaldehyde with ethyl cyanoacetate at 60 °C in $V_{i\text{-propanol}}$:V_{water} = 2 : 1.

The efficiency of the Mg_3Al-PW_{12} composite was also investigated in the case of Knoevenagel condensation of various aldehydes and ketones with malononitrile at 60 °C in $V_{i\text{-propanol}}$:V_{water} = 2 : 1. The obtained data are summarized in Table S6 where it is shown that the corresponding products were obtained at excellent yields.

Table 4. Comparison of yields and TONs for Knoevenagel condensation of benzaldehyde with ethyl cyanoacetate catalyzed by different catalysts.

Entry	Catalyst	Ratio[a]	Solvent	T.(^{o}C)	t(h)	Yield(%)	TON[b]	Ref.
1	Mg_3Al-PW_{12}	47980: 71970: 1	mixed solution[c]	60	8	>99.9	47980	this work
2	VAp[d]	41667: 45833: 1	water	30	5	95	39583	[44]
3	DMAN/SiO_2[e]	10000: 11400: 1	ethanol	60	6	>99.9	10000	[45]
4	polystyrene-supported poly(amidoamine)dendrimer	200: 200: 1	ethanol	50	0.25	99	198	[46]
5	amine-grafted PE-MCM-41[f]	200: 200: 1	cyclohexane	82	1	>99.9	198	[47]
6	[2-aemim]PF_6[g]	125: 125: 1	water	25	3	91	114	[48]
7	functionalized (PS(N_3))-PEG	100: 100: 1	water	20	24	97	97	[49]
8	TBA_4[^{3}-$GeW_{10}O_{34}(H_2O)_2$]	100: 150: 1	acetonitrile	40	0.08	85	85	[50]
9	organic-inorganic hybrid silica material	83: 92: 1	none	130	2	>99.9	83	[51]
10	KOH/La_2O_3-MgO	80: 80: 1	none	25	3	95	76	[52]
11	AP-IL-SBA-15[h]	74: 74: 1	water	50	1	94	70	[53]
12	aminopropyl-functionalized MCM	67: 67: 1	cyclohexane	82	36	94	63	[54]
13	aminopropyl-functionalized SBA-15	55: 55: 1	cyclohexane	82	1	>99	55	[55]
14	LDH-DA[i]	53: 53: 1	DMF	25	2	95	50	[56]
15	LaHAP	50: 75: 1	toluene	60	24	>99	50	[57]
16	$Ru(C_2H_4)(PPh_3)_3$	50: 50: 1	benzene	25	64	98	49	[58]
17	piperidine/microwave irradiation	50: 50: 1	none	25	0.05	96	48	[59]
18	sulfonated nitrocoal acid	50: 50: 1	benzene	reflux	1.5	91	46	[60]

[a] Ratio = n(benzaldehyde): n(ethyl cyanoacetate): n(catalyst); [b] TON (turnover number) = mole of corresponding product/mole of catalyst used; [c] $V_{i\text{-propanol}}$:V_{water} = 2 : 1; [d] VAp = calcium vanadate apatite; [e] DMAN/SiO_2 = 1,8-bis(dimethylamino)naphthalene functionalized SiO_2; [f] PE-MCM-41 = pore-expanded MCM-41; [g] [2-aemim]PF_6 = 1-aminoethyl-3-methylimidazolium hexafluorophosphate; [h] AP-IL-SBA-15 = ionic liquid immobilized on SBA-15; [i] LDH-DA = layered double hydroxides-supported diiospropylamide.

It is worth noting that the Knoevenagel condensation of benzaldehyde and ethyl cyanoacetate gave us a yield of >99.9% using a reaction mixture ratio of benzaldehyde : ethyl cyanoacetate : Mg_3Al-PW_{12} = 47980 : 71970 : 1 at 60 ^{o}C in $V_{i\text{-propanol}}$:V_{water} = 2 : 1. Interestingly, the TON can reach as high as 47980 (Table 4, Entry 1), which is the highest reported so far in comparison with other reported catalysts such as VAp in water (TON = 39583, Entry 2),[44] DMAN/SiO_2 in ethanol (TON = 10000, Entry 3),[45] polystyrene-supported poly(amidoamine)dendrimer in ethanol (TON = 198, Entry 4),[46] amine-grafted PE-MCM-41 in cyclohexane (TON = 198, Entry 5),[47] and others listed in Table 4.[48-60]

In an effort to confirm the fact that the catalysis is truly heterogeneous, the Knoevenagel condensation of benzaldehyde with ethyl cyanoacetate has been selected as an example. After 120 min of reaction, we removed the Mg_3Al-PW_{12} catalyst from the reaction mixture of benzaldehyde and ethyl cyanoacetate by filtration, and the reaction mixture left to proceed under the same conditions (60 ^{o}C, $V_{i\text{-propanol}}$:V_{water} = 2 : 1). As shown in Figure 7A, no product can be obtained by further addition of TMSCN. Moreover, ICP-AES measurement confirmed the absence of Mg, Al, W and P from the filtrate. Taking into consideration the above and our earlier discussed control experiments we can safely rule out the contribution of Mg, Al, W and P-based species due to leaching into the reaction solution. Therefore, the catalytic reaction is truly heterogeneous whilst the catalyst retains its integrity during the course of our studies.

Most importantly, the heterogeneous Mg_3Al-PW_{12} catalyst can be successfully recovered upon completion of the Knoevenagel condensation *via* centrifugation. The yields of the corresponding products remain unchanged upon removal of the catalyst whilst the yield for catalyst recovery is above 96% (Figure 7B). The XRD, FT-IR, solid state NMR, XPS, TPD and BET results confirm further that the structure of the Mg_3Al-PW_{12} remains unchanged (Figure S6 and Table 1). ICP results also reveal that the composition of the reused Mg_3Al-PW_{12} remains

the same (Table S8). All the above data suggest that the structure and composition of Mg_3Al-PW_{12} is not affected during the course of the Knoevenagel condensation and the Mg_3Al-PW_{12} composite is stable before and after the reaction.

Conclusions

To summarize, we demonstrated the successful preparation of a highly efficient Knoevenagel condensation catalyst employing a spontaneous flocculation synthetic approach. More specifically, the traditional Keggin polyoxometalate (PW_{12}) has been successfully intercalated into Mg_3Al-LDHs for the first time using the spontaneous flocculation method, leading to the formation of Mg_3Al-PW_{12} composite. The spontaneous flocculation synthetic approach not only prevents the co-precipitation of impure phases, but also overcomes the spatial and geometrical limitations of PW_{12} intercalation into Mg_3Al-LDHs based on the traditional synthetic way.

Application of Mg_3Al-PW_{12} for the catalysis of Knoevenagel condensation of various aldehydes/ketones with ethyl cyanoacetate / malononitrile at 60 ^oC suggests that the cooperative effect offered by the acidic and basic sites of the Mg_3Al-PW_{12} composite is crucial for the observed highly efficient catalytic activity. To the best of our knowledge, the Mg_3Al-PW_{12}-catalyzed Knoevenagel condensation of benzaldehyde with ethyl cyanoacetate gave the highest TON of 47980 reported so far. The heterogeneous catalyst of Mg_3Al-PW_{12} can be easily recovered and reused for at least ten times without obvious decrease of its catalytic activity. The structural integrity as well as the composition of the Mg_3Al-PW_{12} catalyst remained unaltered during the course of the catalytic reactions.

The facile preparation, reusability and efficacy of the heterogeneous Mg_3Al-PW_{12} catalyst provides great potential for industrial applications. Finally, the straightforward modification by appropriate choice of the polyoxometalate core (architecture and composition) opens the door for further exploration and design of functional materials tailored for specific applications. Our current research effort is focused on exploring the potential of the family of POM-LDHs materials.

Experimental Section

Chemicals: 2-adamantanone (98%), 2-heptanone (97%), 2-octanone (98%), 2-nonanone (98%), 2-decanone (98%), hexanal (99%), heptanal (99%), octanal (98%), nonanal (99%), decanal (96%), benzaldehyde (98%), 2-methylbenzaldehyde (98%), 3-methylbenzaldehyde (97%), 4-methylbenzaldehyde (98%), 2-methoxybenzaldehyde (98%), 3-methoxybenzaldehyde (98%), 4-methoxybenzaldehyde (98%), 2-chlorobenzaldehyde (97%), 3-chlorobenzaldehyde (97%), 4-chlorobenzaldehyde (98%), 2-bromobenzaldehyde (98%), 3-bromobenzaldehyde (97%), 4-bromobenzaldehyde (99%), 2-nitrobenzaldehyde (98%), 3-nitrobenzaldehyde (99%), 4-nitrobenzaldehyde (99%), thiophene-2-carboxaldehyde (98%), pyridine-3-carboxaldehyde (99%), ethyl cyanoacetate (98%), malononitrile (99%), formamide (99%), and all solvents were purchased from Alfa Acesa. Analytical phosphotungstic acid ($H_3PW_{12}O_{40}$), magnesium nitrate ($Mg(NO_3)_2{\cdot}6H_2O$), aluminum nitrate ($Al(NO_3)_3{\cdot}6H_2O$), hexamethylenetetramine (HMT) and nitric acid (65 wt. % HNO_3) were obtained from Energy Chemical in Shanghai. All the chemicals and solvents were used without further purification.

Measurements: X-ray diffraction (XRD) patterns were recorded on a Rigaku XRD-6000 diffractometer under the following conditions: 40 kV, 30 mA, Cu K± radiation (» = 0.154 nm). Fourier transform infrared (FT-IR) spectra were recorded on a Bruker Vector 22 infrared spectrometer using KBr pellet method. Thermogravimetric analysis (TGA) were performed on a TGA/DSC 1/1100 SF from Mettler Toledo in flowing N_2 with a heating rate of 10 $^oC{\cdot}min^{-1}$ from 25 ^oC to 1000 ^oC. Scanning electron microscopy (SEM) images and energy dispersive X-ray (EDX) analytical data were obtained using a Zeiss Supra 55 SEM equipped with an EDX detector. Transmission electron microscopy (TEM) micrographs were recorded using a Hitachi H-800 instrument. Inductively coupled plasma-atomic emission spectroscopy (ICP-AES) analysis was performed using a Shimadzu ICPS-7500 spectrometer. BET measurements were performed at 77 K on a Quantachrome Autosorb-1C analyzer. The samples were degassed at 110 ^oC for 6 hours before the measurements. Solid state NMR measurements were carried out on a Bruker Avance 300 M solid-state spectrometer equipped with a commercial 5 mm MAS NMR probe. X-ray photoelectron spectroscopy (XPS) measurements were performed with monochromatized Al K± exciting X-radiation (PHI Quantera SXM). Temperature-programmed desorption of ammonia (NH_3-TPD) and Temperature-programmed desorption of carbon dioxide (CO_2-TPD) were performed using Auto Chem. II 2920 equipment (Micromeritics, USA). Prior to each test, about 0.05 g of sample was pretreated in He at 350 ^oC for 1 hour, cooled to 100 ^oC and then was saturated with 20% NH_3/He or 40% CO_2/He for 30 min before being purged with He for 30 minutes. Then the sample was heated from 100 to 700 ^oC at a ramp of 10 $^oC{\cdot}min^{-1}$ and the NH_3 or CO_2 desorption was monitored with a TCD detector. The corresponding products were analyzed by Agilent 7820A gas chromatography (GC) system using a 30 m 5% phenylmethyl silicone capillary column with an ID of 0.32 mm and 0.25 µm coating (HP-5). Yields were determined by GC analysis using reference standards. Assignments of corresponding cyanohydrins were analyzed by ^{1}H-NMR and ^{13}C-NMR. ^{1}H-NMR and ^{13}C-NMR spectra was recorded on a Bruker 400 MHz NMR spectrometer.

The preparation method of Mg_3Al-CO_3 and Mg_3Al-NO_3 was reported earlier in the literature.[61] Exfoliation of Mg_3Al-NO_3 was carried out as described.[62]

Preparation of Mg_3Al-PW_{12}: H-PW_{12} (0.23 g, 0.08 mmol) was dissolved in 10 ml H_2O. The Mg_3Al-PW_{12} was synthesized by mixing the exfoliated nanosheets suspension of Mg_3Al-NO_3 and the solution of H-PW_{12} with stirring under N_2 atmosphere for 1 day. The restacked Mg_3Al-PW_{12} composite was isolated by centrifugation, washed with ethanol, water and then dried under vacuum. 0.16 g (Yield = 94%); XRD (Cu K±, ^{o}): 2 Theta = 6.108 (003), 12.148 (006), 28.567 (012), 36.855 (015), 61.094 (110). FT-IR (KBr, cm^{-1}): ½= 3443, 1050, 951, 885, 701, 595, 450. Solid state ^{27}Al-NMR (ppm): 9.15 (AlO_6); Solid state ^{31}P-NMR (ppm): -12.03 (PW_{12}). XPS (eV): 1305.9 (Mg_{1s}), 74.9 (Al_{2p}), 35.6 ($W4f_{7/2}$), 37.7 ($W4f_{5/2}$), 134.3 (P_{2p}). Elemental analysis (%): Found: Mg 9.24, Al 3.01, W 46.49, P 0.71; Cacld. For $Mg_{0.73}Al_{0.22}(OH)_2[PW_{12}O_{40}]_{0.04}$ $0.98H_2O$: Mg 9.32, Al 3.12, W 46.34, P 0.65.

Procedure for Knoevenagel condensation of aldehyeds and ketones: In a typical experiment, 1 mmol aldehyde or ketone, 1.5 mmol methylene compound (ethyl cyanoacetate or malononitrile) and Mg_3Al-PW_{12} (0.25 mol% to substrate based on PW_{12}) as catalyst and 0.6 ml mixed solution (*V*(*i*-propanol): *V*(water) = 2: 1) were added in a 20 ml glass bottle at 60 ^oC whilst the reaction mixture was stirred vigorously. The resulting oily products were extracted by diethyl ether, analyzed by GC, and identified by ^{1}H-NMR and ^{13}C-NMR. The yields were determined by reference standards. After completion of the reaction, the catalysts were recovered *via* centrifugation, washed with acetone, and dried in air.

Acknowledgements

This work was supported by National Basic Research Program (2014CB932104), National Science Foundation of China (21222104, U1407127), the Fundamental Research Funds for the Central Universities (RC1302, YS1406) and Beijing Engineering Center for Hierarchical Catalysts. H.N.M acknowledges the financial support from Univergisity of Glasgow, Royal Society of Edinburgh and Marie Curie actions.

Keywords: polyoxometalates • layered double hydroxides • spontaneous flocculation • Knoevenagel condensation • catalysis

[1] Special issue on “polyoxometalates”, Guest Editor, C. L. Hill, *Chem. Rev.* **1998**, *98*, 1-390.
[2] H. N. Miras, J. Yan, D.-L. Long, L. Cronin, *Chem. Soc. Rev.,* **2012**, *41*, 7403–7430.
[3] a) A. Proust, B. Matt, R. Villanneau, G. Guillemot, P. Gouzerh, G. Izzet, *Chem. Soc. Rev.* **2012**, *41*, 7605-7622; b) B. Schwarz, C. Streb, *Dalton Trans.* **2015**, *44*, 4195-4199.
[4] M. Nymanz, P. C. Burns, *Chem. Soc. Rev.* **2012**, *41*, 7354-7367.
[5] a) Y. F. Song, R. Tsunashima, *Chem. Soc. Rev.* **2012**, *41*, 7384-7402; b) A. Seliverstov, J. Forster, M. Heiland, J. Unfried, C. Streb, *Chem. Commun.* **2014**, *50*, 7840-7843.
[6] a) S. Omwoma, C. T. Gorea, Y. Ji, C. Hu, Y. F. Song, *Coord. Chem. Rev.* **2015**, *286*, 17-29; b) J. Tucher, K. Peuntinger, J. T. Margraf, T. Clark, D. M. Guldi, C. Streb, *Chem. Eur. J.*, **2015**, DOI: 10.1002/chem.201501129.
[7] H. Lv, Y. V. Geletii, C. Zhao, J. W. Vickers, G. Zhu, Z. Luo, J. Song, T. Lian, D. G. Musaev, C. L. Hill, *Chem. Soc. Rev.* **2012**, *41*, 7572-7589.
[8] P. Yin, D. Li, T. Liu, *Chem. Soc. Rev.* **2012**, *41*, 7368-7383.
[9] I. V. Kozhevnikov, Catalysis by Polyoxometalates, Wiley, Chichester, **2002**.
[10] D. L. Long, R. Tsunashima, L. Cronin, *Angew. Chem.* **2010,** *122,* 1780-1803; *Angew. Chem. Int. Ed.* **2010**, *49*, 1736-1758.
[11] D. L. Long, E. Burkholder, L. Cronin, *Chem. Soc. Rev.* **2007**, *126*, 117-123.
[12] N. Mizuno, K. Kamata, K. Yamaguchi, *Top. Catal.* **2010**, *53*, 876-893.
[13] D. E. Katsoulis, *Chem. Rev.* **1998**, *98*, 359-387.
[14] W. Qi, Y. Wang, W. Li, L. Wu, *Chem. Eur. J.* **2010**, *16*, 1068-1078.
[15] C. Hu, D. Li, in: F. Wypych (Ed.), Clay Surfaces: Fundamentals and Applications, Elsevier Inc., San Diego, **2004**, pp. 374-402.
[16] V. Rives, D. Carriazo, C. Martin, in: A. Gill, S. A. Korili, R. Trujillano, M. A. Vicentè (Eds.), Pillared Clays and Related Catalysis, Springer, New York, **2010**, pp. 319-422.
[17] N. Mizuno, K. Yamaguchi, K. Kamata, *Catal. Surv. Asia* **2011**, *15*, 68-79.
[18] F. Cavani, F. Trifiró, A. Vaccari, *Catal. Today* **1991**, *11*, 173-301.
[19] V. Rives, M. A. Ulibarr, *Coord. Chem. Rev.* **1999**, *181*, 61-120.
[20] G. Fan, F. Li, D. G. Evans, X. Duan, *Chem. Soc. Rev.* **2014**, *43*, 7040-7066.
[21] X. Duan, D. G. Evans, Structure and Bonding, Springer-Verlag, Berlin Heidelberg, **2006**, pp. 1-223.
[22] Q. Wang, D. O’Hare, *Chem. Rev.* **2012**, *112*, 4124-4155.
[23] M. Osada, T. Sasaki, *Adv. Mater.* **2012**, *24*, 210-288.
[24] C. Yu, J. He, *Chem. Comm.* **2012**, *48*, 4933-4940.
[25] S. K. Yun, T. J. Pinnavaia, *Inorg. Chem.* **1996**, *35*, 6853-6860.
[26] B. Sels, D. De Vos, M.. Buntinx, F. Pierard, A. Kirsch-De Mesmaeker, P. A. Jacobs, *Nature* **1999**, *400*, 855-857.
[27] P. Liu, C. Wang, C. Li, *J. Catal.* **2009**, *262*, 159-168.
[28] S. Zhao, J. Xu, M. Wei, Y. F. Song, *Green Chem.* **2011**, *13*, 384-389.
[29] B. F. Sels, D. E. De Vos, P. A. Jacobs, *Catal. Rev.* **2001**, *43*, 443-488.
[30] S. Omwoma, W. Chen, R. Tsunashima, Y. F. Song, *Coord. Chem. Rev.* **2014**, *258-259*, 58-71.
[31] T. Kwon, T. J. Pinnavaia, *J. Mol. Catal.* **1992**, *74*, 23-33.
[32] Y. Jia, S. Zhao, Y. F. Song, *Appl. Catal. A: Gen.* **2014**, *487*, 172-180.
[33] N. Iyi, H. Yamada, T. Sasaki, *Appl. Clay Sci.* **2011**, *54*, 132-137.
[34] Z. Han, Y. Guo, R. Tsunashima, Y. F. Song, *Eur. J. Inorg. Chem.* **2013**, *9*, 1475-1480.
[35] Y. Chen, D. Yan, Y. F. Song, *Dalton Trans.* **2014**, *43* 14570-14576.
[36] Y. Zhao, F. Li, R. Zhang, D. G. Evans, X. Duan, *Chem. Mater.* **2002**, *14*, 4286-4291.
[37] K. Nakamoto, *Infrared and Raman Spectra of Inorganic and Coodination Compounds*, 4th ed.; John Wiely and Sons: New York, **1986**, 137-141.
[38] J. T. Kloprogge, R. L. Frost, *J. Solid State Chem.* **1999**, *146*, 506-515.
[39] Z. P. Xu, H. C. Zeng, *Chem. Mater.* **2001**, *13*, 4555-4563.
[40] K. S. W. Sing, D. H. Everett, R. A. W. Haul, L. Moscou, R. A. Pierotti, J. Rouquerol, T. Siemieniewska, *Pure Appl*. *Chem.* **1985**, *57*, 603-620.
[41] L. F. Tietze, U. Beifuss, in Comprehensive Organic Synthesis, Editor B. M. Trost, I. Fleming, C. H. Heathcock, Pergamon Press, Oxford, **1991**, *2*, 341–392.
[42] F. Bigi, L. Chesini, R. Maggi, G. Sartori, *J. Org. Chem.* **1999**, *64***,** 1033-1035.
[43] N. Yu, J. M. Aramini, M. W. German, Z. Huang, *Tetrahedron Lett.* **2000**, *41***,** 6993-6996.
[44] T. Hara, S.Kanai, K. Mori, T. Mizugaki, K. Ebitani, K. Jitsukawa, K. Kaneda, *J. Org. Chem.* **2006**, *71*, 7455-7462.
[45] E. Gianotti, U. Diaz, S. Coluccia, A. Corma, *Phys. Chem. Chem. Phys.* **2011**, *13*, 11702-11709.
[46] G. R. Krishnan, K. Sreekumar, *Eur. J. Org. Chem.* **2008**, 4763-4768.
[47] D. D. Das, P. J. E. Harlick, A. Sayari, *Catal. Commun.* **2007**, *8*, 829-833.
[48] Y. Cai, Y. Peng, G. Song, *Catal. Lett.* **2006**, *109*, 61-64.
[49] V. Rodionov, H. Gao, S. Scroggins, D. A. Unruh, A. J. Avestro, J. M. J. Fréchet, *J. Am. Chem.Soc.* **2010**, *132*, 2570-2572.
[50] K. Sugahara, T. Kimura, K. Kamata, K. Yamaguchi, N. Mizuno, *Chem. Comm.* **2012**, *48*, 8422-8424.
[51] M. Trilla, R. Pleixats, M. W. C. Man, C. Bied, *Green Chem.* **2009**, *11*, 1815-1820.
[52] A. Kumar, M. Dewan, A. Saxena, A. De, S. Mozumdar, *Catal. Commun.* **2010**, *11*, 679-683.
[53] H. Zhao, N. Yu, Y. Ding, R. Tan, C. Liu, D. Yin, H. Qiu, D. Yin, *Micropor. Mesopor. Mater.* **2010**, *136*, 10-17.
[54] D. J. Macquarrie, D. B. Jackson, *Chem. Commun.* **1997**, 1781-1782.
[55] X. Wang, K. S. K. Lin, J. C. C. Chan, S. Cheng, *J. Phys. Chem. B* **2005**, *109*, 1763-1769.
[56] M. L. Kantam, A. Ravindra, C. V. Reddy, B. Sreedhar, B. M. Choudary, *Adv. Synth. Catal.* **2006**, *348*, 569-578.
[57] K. Mori, M. Oshiba, T. Hara, T. Mizugaki, K. Ebitani, K. Kaneda, *New J. Chem.* **2006**, *30*, 44-52.
[58] Y. Mizuho, N. Kasuga, S. Komiya, *Chem Lett.* **1991**, 2127-2130.
[59] S. A. E. Ayoubi, F. Texier-Boullet, J. Hamelin, *Synthesis* **1994**, *3*, 258-260.
[60] C. K. S. Nair, M. Pardasaradhi, *Fuel* **1995**, *74*, 1531-1532.
[61] N. Iyi, Y. Ebina, T. Sasaki, *J. Mater. Chem.* **2011**, *21*, 8085-8095.
[62] Z. Liu, R. Ma, M. Osada, N. Iyi, Y. Ebina, K. Takada, T. Sasaki, *J. Am. Chem. Soc.* **2006**, *128*, 4872-4880.